McGarry, B., Rogers, H., Knight, M. J., Jokivarsi, K. T., Sierra, A., Grohn, O. H. J., & Kauppinen, R. A. (2016). Stroke onset time estimation from multispectral quantitative magnetic resonance imaging in a rat model of focal permanent cerebral ischaemia. International Journal of Stroke, 11(6), 677-682. DOI: 10.1177/1747493016641124

Stroke onset time estimation from multispectral quantitative magnetic resonance imaging in a rat model of focal permanent cerebral ischaemia

Journal:	*International Journal of Stroke*
Manuscript ID	IJS-10-15-4497.R1
Manuscript Type:	Research
Date Submitted by the Author:	n/a
Complete List of Authors:	McGarry, Bryony Rogers, Harriet Knight, Michael Jokivarsi, Kimmo; University of Eastern Finland, Department of Neubiology Sierra-Lopez, Alejandra; University of Eastern Finland, Department of Neurobiology Grohn, Olli; University of Eastern Finland, Department of Neurobiology Kauppinen, Risto; University of Bristol, School of Experimental Psychology
Keywords:	Ischaemic stroke, MRI, Methodology, Acute, Brain, Cerebral Infarction

Stroke onset time estimation from multispectral quantitative magnetic resonance imaging in a rat model of focal permanent cerebral ischaemia

Bryony L. McGarry[1], Harriet J. Rogers[1], Michael J. Knight[1], Kimmo T. Jokivarsi[2], Alejandra Sierra[2], Olli H.J. Grohn[2] and Risto A. Kauppinen[1]

[1] School of Experimental Psychology and Clinical Research and Imaging Centre Bristol, University of Bristol, Bristol, UK.

[2] Department of Neurobiology, A.I. Virtanen Institute, University of Eastern Finland, Kuopio, Finland.

Correspondence:

Professor Risto Kauppinen
University of Bristol
School of Experimental Psychology
12a Priory Road, Clifton
Bristol, BS8 1TU
Tel + 44 – 117 928 8461
e-mail psrak@bristol.ac.uk

Key words: Ischaemic stroke, MRI, T_1 and T_2 MRI, onset time

Word Count: 3999

ABSTRACT

Background: Quantitative T_2 (qT_2) relaxation Magnetic Resonance Imaging (MRI) allows estimation of stroke onset time.

Aims: We aimed to examine the accuracy of quantitative T_1 (qT_1) and qT_2 relaxation times alone and in combination to provide estimates of stroke onset time in a rat model of permanent focal cerebral ischaemia and map the spatial distribution of elevated qT_1 and qT_2 to assess tissue status.

Methods: Permanent middle cerebral artery occlusion (MCAo) was induced in Wistar rats. Animals were scanned at 9.4T for qT_1, qT_2 and Trace of Diffusion Tensor (D_{av}) up to 4 hours post MCAo. Time courses of differentials of qT_1 and qT_2 in ischaemic and non-ischaemic contralateral brain tissue (ΔT_1, ΔT_2) and volumes of tissue with elevated T_1 and T_2 relaxation times (f_1 , f_2) were determined. TTC staining was used to highlight permanent ischaemic damage.

Results: ΔT_1, ΔT_2,f_1 , f_2 and the volume of tissue with both elevated qT_1 and qT_2 ($V^{Overlap}$) increased with time post MCAo allowing stroke onset time to be estimated. $V^{Overlap}$ provided the most accurate estimate with an uncertainty of ±25 minutes. At all times-points regions with elevated relaxation times were smaller than areas with D_{av} defined ischaemia.

Conclusions: Stroke onset time can be determined by qT_1 and qT_2 relaxation times and tissue volumes. Combining qT1 and qT_2 provides the most accurate estimate and potentially identifies irreversibly damaged brain tissue.

INTRODUCTION

A growing body of evidence shows quantitative ^{1}H MRI is sensitive to changes in brain tissue that occur during early moments of an ischaemic stroke and can enable identification of patients with an unknown onset time who may be eligible for drug therapies (1–3). Research from preclinical stroke models and stroke patients suggest MRI can provide an estimate of stroke onset time (1–4) and a means for assessing tissue status (4–6), two methods that could aid stratification of patients to treatment.

Within minutes of ischaemia onset, the apparent diffusion coefficient (ADC by quantitative diffusion MRI) has been shown to decrease to approximately 60% of physiological values in brain parenchyma, enabling ischaemic tissue to be identified (7–10), thereafter stabilizing(14) (15). This early ADC decrease is attributed to energy failure and cytotoxic oedema (7,8) and is often assumed to represent the irreversibly infarcted core (11), however preclinical (12) and clinical (13) studies suggest greater complexity.

Within regions of decreased ADC in rat focal ischaemia, quantitative T_2 relaxation times (qT_2) also decrease due to metabolic changes (6,16) and cytotoxic oedema (17). The decrease is followed by a quasi-linear increase over time (2,4) caused by altered hydrodynamics and tissue degradation (17,18). This relationship between qT_2 and time from stroke onset has enabled estimates of stroke onset time in rat models of ischaemia with good accuracy (2,4). Interestingly, a quadratic dependency of qT_2 and time from symptom onset was also reported in acute stroke patients suggesting clinical applicability of qT_2 MRI (3). Over time, the qT_2 increase will have inevitable contributions from vasogenic oedema, which coincides with the transition to irreversible tissue damage (6,9,14).

The time-dependency of quantitative T_1 relaxation times (qT_1) in the ischaemic brain is less well characterized. qT_1 increases gradually over time from stroke onset within regions of decreased diffusion (16,9). Pathophysiological mechanisms thought to underlie this qT_1 increase are similar to qT_2, including altered water dynamics and content in ischaemic tissue (14,19) qT_1 is additionally sensitive to changes in cerebral blood flow and volume (16,20), temperature (21), pH (22) and tissue oxygen tension (16). Thus, by combining data from time courses of qT_1 and qT_2 in the ADC lesion, one would expect to obtain a fuller picture of

ischaemic pathology in brain tissue, which may aid in the estimation of stroke onset and assessment of tissue viability.

The current study was undertaken to determine time-dependent changes in qT_1 and qT_2 relaxation times in ischaemic brain tissue and to compare their abilities in estimating time since stroke onset. The second aim was to map the spatial distributions of elevated qT_1 and qT_2 relaxation times within regions of decreased ADC with a view to assessing tissue status. Given that these MRI parameters are influenced by the same and different pathophysiological changes during stroke, ischaemic areas with combinations of qT_1 and qT_2 signatures were also identified. Previous research (4,9,17,23) has shown that the volume of tissue with elevated relaxation times increase with time. Therefore we also quantified the volumes of tissue with elevated qT_1 and qT_2 in the ADC lesion as a function of time.

METHODS

Animal Model

Animal procedures were conducted according to the principles of Three Rs and European Community Council Directives 86/609/EEC guidelines and approved by the Animal Care and Use Committee of the University of Eastern Finland.

Five male Wistar rats (300 – 400 g, Animal Resource Facility, University of Eastern Finland, Kuopio, Finland) underwent permanent middle cerebral artery occlusion (MCAo) (24). All rats were anesthetized with isoflurane through a facemask (maintained at 1.5 – 2.4%) for the duration of the operation and MRI. Before MRI arterial blood gases and pH were analysed (i-Stat CO, East Windsor, NJ). During MRI breathing rate and rectal temperature were monitored. Core temperature was maintained close to 37°C using a water heating pad under the torso.

One rat died during MRI (~ 3.5 hours post MCAo) and others were sacrificed five hours after MCAo by decapitation in deep isoflurane anaesthesia. Following decapitation, the brain was extracted, placed in refrigerated 0.01M phosphate buffered saline and sectioned into 1mm axial slices. Immediately after sectioning, a Triphenyletrazolium chloride (TTC 0.5% or 1% in phosphate buffered saline) staining method (25) was used to confirm ischaemic damage to brain tissue.

Magnetic Resonance Imaging

MRI data were acquired using a 9.4T/31cm horizontal Varian magnet interfaced to a Direct Drive console (Agilent Inc., Palo Alto, CA, USA) and equipped with an actively decoupled linear volume transmitter and quadrature receiver coil pair (RAPID Biomedical GmbH, Rimpar, Germany). Immediately after MCAo rats were secured in a cradle at the centre of the magnet bore. Protocol included twelve axial slices of: the trace of diffusion tensor (D_{av}= 1/3 trace [D]) with three bipolar gradients along each axis, three b-values (0, 400 and 1400 s/mm^2), TE = 36 ms, TR = 4000 ms and acquisition time = 7.36 minutes, a Carr-Purcell-Meiboom-Gill T_2 sequence with 12 echoes (echo-spacing = 10 ms, TR = 2000 ms, acquisition time = 4.20 minutes) and Fast Low Angle Shot (FLASH) for T_1, where the time from inversion to the first FLASH sequence (T_{10}) was 7.58 ms, TI = 600 ms, TR = 5.5 ms, time between inversion pulses (T_{relax}) = 10 s and acquisition time = 8.20 minutes. MRI data were

congruently sampled with slice-thickness = 1 mm, slice-gap = 0.5 mm, field-of-view = 2.56 x 2.56 cm^2, matrix = 128 x 128. MRI data were acquired sequentially at 60, 120, 180 and 240 minutes after MCAo.

Image Post-processing and Data Analysis

Data analysis was performed using Matlab (MathWorks, Natick, Massachusetts, USA) scripts written in-house and MRI software 'Mango' (Research Imaging Institute, UT Health Science Center at San Antonio, Texas, USA) and 'FSL' (FMRIB, Oxford UK). See Supplementary Materials for specific details of methods and criteria used.

Quantitative maps were computed using a mono-exponential fit in a logarithmic space (26). Ischaemic tissue was identified and ischaemic volumes of interest (VOI) were generated by applying Knight et al.'s (17) automatic lesion detection method to reciprocal Dav images (1/Dav). Reflecting ischaemic VOIs about the vertical axis identified homologous regions in the non-ischaemic hemisphere. To quantify changes in relaxation times, the percentage difference in mean qT_1 and qT_2 between ischaemic and non-ischaemic VOIs were calculated (ΔT_1 and ΔT_2). To picture the spatial distribution of elevated relaxation time changes within ischaemic VOIs, voxels with high qT_1 or qT_2 and voxels with both high qT_1 and qT_2, termed T_1 & T_2 Overlap, were colour-coded. Voxels were high if relaxation times exceeded the median relaxation time of the non-ischaemic VOI by more than one half-width at half maximum. To determine the size of the lesion according to T_1 and T_2, parameter f, as introduced by Knight et al. (17) was computed. Where f_1 and f_2 represent the number of voxels with high T_1 or T_2 (respectively) as a percentage of the size of the ischaemic VOI. The extent of T_1 & T_2 Overlap was determined by calculating the volume of T_1 & T_2 Overlap ($V^{Overlap}$) as a percentage of whole-brain volume.

Statistical Analysis

Statistical analysis was performed using Matlab and IBM Statistical Package for the Social Sciences (SPSS) Version 21 (Armonk, NY: IBM Corp) on pooled rat data. To compare lesion sizes, one-way related ANOVAs and Fisher's least significant difference post-hoc were conducted on the average number of voxels in ischaemic VOI and with high qT_1 and qT_2. Differences were considered significant at $p < .05$. Linear least square regression analyses

were performed to determine whether time since stroke onset could be predicted by quantifying a parameter of interest (ΔT_1, ΔT_2, f_1 , f_2 , $V^{Overlap}$) at a single time-point. The root mean square error (RMSE) was used to assess the accuracy of onset time estimates. To compare the magnitude of ΔT_1 and ΔT_2, average ΔT_1 and ΔT_2 at 3 hours post MCAo were estimated using trend-line equations.

RESULTS

Across rats the blood gas profiles were: SO_2 = 95.8±3.2%, P_aCO_2 = 51.6±2.9 mmHg and pH = 7.30±0.04. In agreement with previous reports at 9.4T (33), mean qT_1 and qT_2 of the non-ischaemic VOI were 2,023±116 ms and 47±1 ms respectively. Figure 1 shows a central $1/D_{av}$, qT_2 and qT_1 MRI slices of a representative rat at each time-point and a TTC slice. It should be pointed out that both in qT_2 and qT_1 MR images ischaemic stroke causes increased brightness with time, whereas in T_2 and T_1-weighted images stroke lesion becomes brighter and darker, respectively. TTC staining verified irreversible ischaemic damage located predominantly in gray matter in all rats.

Figure 2 shows the spatial distribution of elevated relaxation times within ischaemic VOIs during the first four hours of ischaemia. As seen, the extent of T_1 & T_2 Overlap increases with time and at all time-points regions with high qT_1 and qT_2 appear smaller than the ischaemic VOI. Regions of high qT_1 also appear larger than and occur in different regions to high qT_2 areas.

At one and two hours post MCAo, regions with high qT_1 were significantly larger than high qT_2 and the ischaemic VOI was larger than high qT_1 and high qT_2 although this latter difference just missed significance for qT_1 at two hours (p = .058). There was no difference between lesion sizes of all parameters at three hours post MCAo and at four hours, the ischaemic VOI was significantly larger than high qT_2. Overall, in the initial hours of ischaemia, regions of decreased diffusion ($1/D_{av}$ Ischaemic VOI) were larger than regions with high qT_1 and qT_2 and regions with high qT_1 were larger than regions with high qT_2 but converged with time.

As shown in Figure 3, all parameters (ΔT_1, ΔT_2, f_1 , f_2 , $V^{Overlap}$) were significant predictors

of tMCAo ($p < .001$), which enabled estimates of stroke onset time using linear trend-line equations (see Figure 3). $V^{Overlap}$ was the strongest predictor (R^2 = 0.87) and provided the most accurate estimate of time since stroke onset, with an uncertainty of ± 25 min. f_2 (R^2 = 0.82) and ΔT_2 (R^2) = 0.75, had uncertainties of ±34 and ±28 minutes, respectively. The increase in ΔT_1 (R^2 = 0.71) and f_1 (R^2 = 0.53) over time were more gradual than other parameters and thus uncertainties were higher, at ±37 minutes and ±47 minutes for f_1 respectively. At 3 hours post MCAo the average ΔT_1 was +6% and ΔT_2 +5%.

DISCUSSION

Both ΔT_1 and ΔT_2 relaxation times provided estimates of stroke onset time where ΔT_2 was superior to ΔT_1. The volume of tissue with elevated qT_1 and qT_2 (f_1 , f_2) also increased with stroke duration and quantification of $V^{Overlap}$ enabled estimates of onset time with better accuracy than individual measures. The ability to estimate stroke onset time by ^{1}H MRI is regarded beneficial for patients with unknown onset, as currently they are ineligible for thrombolytic therapy (27). The fact that the volume of elevated relaxation times was smaller than regions of reduced D_{av} indicates MRI relaxometry may also be informative of tissue status in hyperacute stroke.

The increase in qT_2 with tMCAo and its utility in estimating stroke onset time agrees with preclinical studies using single-slice MRI data acquisition (2,4) and a clinical study with multi-slice acquisition (3). Previous studies have reported a qT_1 increase in hyperacute ischeamia (16,9) but this study is the first to identify qT_1 as a significant predictor of time from ischaemia onset and thus, a potential proxy for stroke timing. We introduce f_1 and f_2 parameters as indices for abnormal qT_1 and qT_2 relaxation times in the ischaemic tissue to eliminate MRI technical shortcomings, including magnetic field variation within the lesion (17). A combination of these parameters, $V^{Overlap}$, provided the most accurate estimate of stroke duration thus motivating further exploration as a proxy for onset time.

While both qT_1 and qT_2 enabled stroke onset time to be estimated, qT_1 had higher levels of uncertainty, which is likely to be due to the shallow slope of ΔT_1 vs. time plot (Figure 3D). Previous studies showed within the ADC lesion, qT_1 and qT_2 (5,6) change in opposite

directions in the early moments of ischaemia; qT_1 increases within the first minute (20) and qT_2 decreases for about an hour (5,6). Recent data point to two-phase response of qT_1 upon ischaemia onset; in complete forebrain ischaemia the fast response levels by two minutes (20) whereas in the core, the rapid increase lasts up to 25 minutes post MCAo (16). A further issue to be considered is that inherent qT_1 and qT_2 change with magnetic field strength. For example a previous study found after 10 minutes of ischaemia the ΔT_1 was approximately two-fold greater at 9.4T than 4.7T (20). However at three hours post MCAo, ΔT_1 of a similar magnitude has been determined; at 4.7T the ΔT_1 was +9% (8) and here at 9.4T, it was +6%. In contrast to ΔT_1, in the early moments of ischaemia ΔT_2 is negative in the core (2,6) and becomes positive after an hour at both 4.7T (2,4) and 9.4T. The initial negative ΔT_2 is likely to be due to combined effects of deoxyhaemoglobin build up (6) and cytotoxic oedema (17). However, at three hours of MCAo ΔT_2 are similar at 4.7T (+5%) (2) and 9.4T (+5%) (Figure 3E) in the core of ischaemia. These observations indicate that while the polarity of early changes and time-dependent kinetics of qT_1 and qT_2 differ in stroke tissue, the increases in both relaxation times at clinically relevant time-points are comparable and independent of magnetic field strength.

The spatial distribution of elevated relaxation times (Figure 2) and the f_1 and f_2 parameters revealed that the volume of tissue with elevated qT_1 is initially larger than the volume of tissue with elevated qT_2, but these volumes converge with time. This observation agrees with a recent report (23), where at 70 and 150 minutes post MCAo the qT_1 lesion area was significantly larger than the qT_2 lesion, but comparable at 24 hours. Anatomical differences in volumes with elevated qT_1 and qT_2 may reflect the fact that these relaxation times probe different factors of early stroke pathophysiology, yet some of the same mechanisms during later stages of ischaemia (18). In line with earlier studies (4,9), volumes of tissue with elevated qT_1 and qT_2 were smaller than those with low diffusion during the initial hours of ischaemia. Close to normal qT_1 and qT_2 values are observed in early moments before transition to irreversible ischaemia (14). Thus present findings support current notions that diffusion MRI overestimates the true extent of the ischaemic core (4,12,13). Combining qT_1 and qT_2 and ADC data may provide a method for identifying salvageable tissue, where 'normal' qT_1 and qT_2 in the presence of decreased ADC could indicate tissue viability.

Increased qT_2 and low ADC represents irreversible tissue damage (5,6,10,14). The viability

of tissue with elevated qT_1 is unknown, but it was previously reported that in transient MCAo of 90 minutes, qT_1 normalised in the striatum and core upon reperfusion, but the striatum proceeded to infarction two days later (20). We therefore speculate that volumes with **both** elevated qT_1 and qT_2 relaxation times, $V^{overlap}$, represent irreversibly damaged tissue. This conclusion is supported by the fact that prolonged qT_1 and qT_2 times in ischaemic brain were shown to signify transition to necrosis by histological methods (14). We believe that $V^{Overlap}$ represents tissue with irreversible vasogenic oedema and thus, increased total water content as both qT_1 and qT_2 are influenced by total tissue water content (19).

To conclude, the present study indicates that quantification of absolute T_1 and T_2 relaxation times and $V^{overlap}$ could provide information about tissue status and onset time that would be invaluable for treatment stratification of acute stroke patients with unknown onset.

ACKNOWLEDGEMENTS

Expert technical assistance by Mrs Maarit Pulkkinen is greatly appreciated.

FUNDING

BLM and HJR received a travel grant to University of Eastern Finland from the School of Experimental Psychology, University of Bristol. MJK is funded by Alzheimer's Research UK and BRACE Charity. AS, KJ and OG are funded by Academy of Finland, UEF-Brain strategic funding from University of Eastern Finland and by Biocenter Finland

CONFLICT OF INTEREST

The authors declare no conflicts of interest.

REFERENCES

1. Thomalla G, Rossbach P, Rosenkranz M, Siemonsen S, Krützelmann A, Fiehler J, et al. Negative fluid-attenuated inversion recovery imaging identifies acute ischemic stroke at 3 hours or less. Ann Neurol. 2009;65:724–32.

2. Jokivarsi KT, Hiltunen Y, Gröhn H, Tuunanen P, Gröhn OH, Kauppinen RA. Estimation of the Onset Time of Cerebral Ischemia Using T1ρ and T2 MRI in Rats. Stroke. 2010;41:2335–40.

3. Siemonsen S, Mouridsen K, Holst B, Ries T, Finsterbusch J, Thomalla G, et al. Quantitative t2 values predict time from symptom onset in acute stroke patients. Stroke J Cereb Circ. 2009; 40:1612–6.

4. Rogers HJ, McGarry BL, Knight MJ, Jokivarsi KT, Gröhn OHJ, Kauppinen RA. Timing the ischaemic stroke by 1H-MRI: improved accuracy using absolute relaxation times over signal intensities. NeuroReport. 2014; 25:1180-5.

5. Jokivarsi KT, Hiltunen Y, Tuunanen PI, Kauppinen RA, Gröhn OH. Correlating tissue outcome with quantitative multiparametric MRI of acute cerebral ischemia in rats. J Cereb Blood Flow Metab. 2009; 11; 30:415–27.

6. Gröhn OHJ, Lukkarinen JA, Oja JME, van Zijl PCM, Ulatowski JA, Traystman RJ, et al. Noninvasive Detection of Cerebral Hypoperfusion and Reversible Ischemia From Reductions in the Magnetic Resonance Imaging Relaxation Time, T2. J Cereb Blood Flow Metab. 1998; 18:911–20.

7. Moseley ME, Cohen Y, Mintorovitch J, Chileuitt L, Shimizu H, Kucharczyk J, et al. Early detection of regional cerebral ischemia in cats: comparison of diffusion- and T2-weighted MRI and spectroscopy. Magn Reson Med Off J Soc Magn Reson Med Soc Magn Reson Med. 1990; 14:330–46.

8. Moonen CT, Pekar J, de Vleeschouwer MH, van Gelderen P, van Zijl PC, DesPres D. Restricted and anisotropic displacement of water in healthy cat brain and in stroke studied by NMR diffusion imaging. Magn Reson Med. 1991; 19:327–32.

9. Hoehn-berlarge M, Eis M, Back T, Kohno K, Yamashita K. Changes of relaxation times (T1, T2) and apparent diffusion coefficient after permanent middle cerebral artery occlusion in the rat: temporal evolution, regional extent, and comparison with histology. Magn Reson Med. 1995; 34:824–34.

10. Hoehn-Berlage M, Norris DG, Kohno K, Mies G, Leibfritz D, Hossmann K-A. Evolution of Regional Changes in Apparent Diffusion Coefficient During Focal Ischemia of Rat Brain: The Relationship of Quantitative Diffusion NMR Imaging to Reduction in Cerebral Blood Flow and etabolic Disturbances. J Cereb Blood Flow Metab. 1995; 15:1002–11.

11. Burgess RE, Kidwell CS. Use of MRI in the Assessment of Patients with Stroke. Curr Neurol Neurosci Rep. 2011; 11:28–34.

12. Kohno K, Hoehn-Berlage M, Mies G, Back T, Hossmann K-A. Relationship between diffusion-weighted MR images, cerebral blood flow, and energy state in experimental brain infarction. Magn Reson Imaging. 1995; 13:73–80.

13. Kranz PG, Eastwood JD. Does Diffusion-Weighted Imaging Represent the Ischemic Core? An Evidence-Based Systematic Review. Am J Neuroradiol. 2009; 30:1206–12.

14. Knight RA, Dereski MO, Helpern JA, Ordidge RJ, Chopp M. Magnetic resonance imaging assessment of evolving focal cerebral ischemia. Comparison with histopathology in rats. Stroke. 1994; 25:1252–61.

15. Madai VI, Galinovic I, Grittner U, Zaro-Weber O, Schneider A, Martin SZ, et al. DWI Intensity Values Predict FLAIR Lesions in Acute Ischemic Stroke. PLoS ONE. 2014; 9(3):e92295.

16. Calamante F, Lythgoe MF, Pell GS, Thomas DL, King MD, Busza AL, et al. Early changes in water diffusion, perfusion, T1, and T2 during focal cerebral ischemia in the rat studied at 8.5 T. Magn Reson Med. 1999; 41:479–85.

17. Knight MJ, McGarry B., Rogers, Jokivarsi. A spatiotemporal theory for MRI T2 relaxation time and apparent diffusion coefficient in the brain during acute ischaemia: Application and validation in a rat acute stroke model. J Cereb Blood Flow Metab. 2015; 10.1177/0271678X15608394

18. Kauppinen RA. Multiparametric magnetic resonance imaging of acute experimental brain ischaemia. Prog Nucl Magn Reson Spectrosc. 2014; 80:12–25.

19. Kato H, Kogure K, Ohtomo H, Izumiyama M, Tobita M, Matsui S, et al. Characterization of Experimental Ischemic Brain Edema Utilizing Proton Nuclear Magnetic Resonance Imaging. J Cereb Blood Flow Metab. 1986; 6:212–21.

20. Kettunen MI, Gröhn OHJ, Lukkarinen JA, Vainio P, Silvennoinen MJ, Kauppinen RA. Interrelations of T1 and diffusion of water in acute cerebral ischemia of the rat. Magn Reson Med. 2000; 44:833–9.

21. Youl BD, Hawkins CP, Morris JK, DuBoulay EP, Tofts PS. In vivo T1 values from guinea pig brain depend on body temperature. Magn Reson Med Off J Soc Magn Reson Med Soc Magn Reson Med. 1992; 24:170–3.

22. Kettunen MI, Gröhn OHJ, Silvennoinen MJ, Penttonen M, Kauppinen RA. Effects of intracellular pH, blood, and tissue oxygen tension on T1ρ relaxation in rat brain. Magn Reson Med. 2002; 48:470–7.

23. Kaur J, Tuor UI, Zhao Z, Petersen J, Jin AY, Barber PA. Quantified T1 as an adjunct to apparent diffusion coefficient for early infarct detection: a high-field magnetic resonance study in a rat stroke model. Int J Stroke. 2009; 4:159–68.

24. Longa EZ, Weinstein PR, Carlson S, Cummins R. Reversible middle cerebral artery occlusion without craniectomy in rats. Stroke J Cereb Circ. 1989; 20:84–91.

25. Joshi CN, Jain SK, Murthy PSR. An optimized triphenyltetrazolium chloride method for identification of cerebral infarcts. Brain Res Protoc. 2004; 13:11–7.

26. Nekolla S, Gneiting T, Syha J, Deichmann R, Haase A. T1 maps by K-space reduced snapshot-FLASH MRI. J Comput Assist Tomogr. 1992; 16:327–32.

27. Hacke W, Kaste M, Bluhmki E, Brozman M, Dávalos A, Guidetti D, et al. Thrombolysis with alteplase 3 to 4.5 hours after acute ischemic stroke. N Engl J Med. 2008; 359:1317–29.

Legends to Figures:

Figure 1 (colour). A single representative slice from a typical rat shown as 1/Dav, qT_2 and qT_1 images over tMCAo and a TTC stained slice from the same rat verifying irreversible ischaemic damage five hours post MCAo.

Figure 2 (colour). A central 1/Dav slice from the same representative rat in Figure 1 shown over tMCAo. The image remains the same in the x direction and is overlaid with colour-coded regions depicting the 1/Dav defined ischaemic VOI, areas with high qT_2, high qT_1 and T_1 & T_2 Overlap.

Figure 3 (colour). MRI parameters as a function of tMCAo. ΔT_1 and ΔT_2 represent the percentage difference between the ischaemic and non-ischaemic hemispheres. **A:** f_1 , where tMCAo = 13.16 (±6.40) *f_1 – 999.15 (±558.5). **B:** f_2 , where tMCAo = 3.449 (± 0.817) * f_2 – 110.90 (± 64.00). **C:** $V^{overlap}$, where tMCAo =37.41 (± 14.92) * $V^{overlap}$ + 50.52(± 22.47). **D:** ΔT_1, where tMCAo = 42.83 (± 13.88) * ΔT_1 – 93.03 (± 83.17). **E:** ΔT_2 where tMCAo = 24.41 (± 7.2) * ΔT_2 + 64.74 (± 30.86).

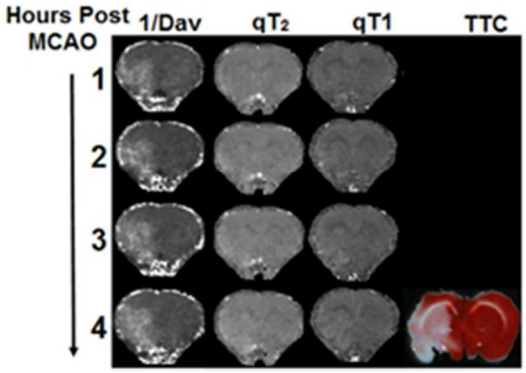

Figure 1 (colour). A single representative slice from a typical rat shown as 1/Dav, qT2 and qT1 images over tMCAo and a TTC stained slice from the same rat verifying irreversible ischaemic damage five hours post MCAo.
22x16mm (300 x 300 DPI)

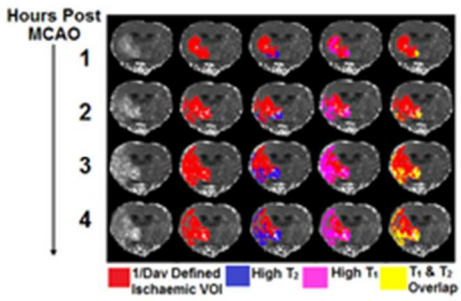

Figure 2 (colour). A central 1/Dav slice from the same representative rat in Figure 1 shown over tMCAo. The image remains the same in the x direction and is overlaid with colour-coded regions depicting the 1/Dav defined ischaemic VOI, areas with high qT2, high qT1 and T1 & T2 Overlap.
19x12mm (300 x 300 DPI)

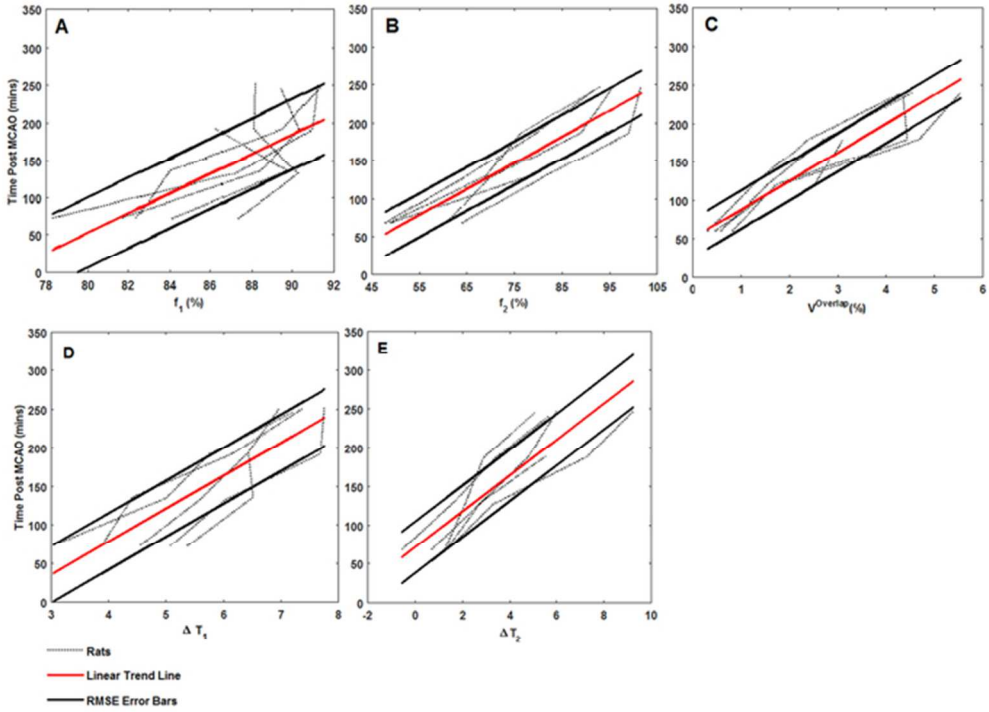

Figure 3 (colour). MRI parameters as a function of tMCAo. ΔT1 and ΔT2 represent the percentage difference between the ischaemic and non-ischaemic hemispheres. A: f_(1), where tMCAo = 13.16 (±6.40) *f_(1) – 999.15 (±558.5). B: f_(2), where tMCAo = 3.449 (± 0.817) * f_(2) – 110.90 (± 64.00). C: Voverlap, where tMCAo =37.41 (± 14.92) * Voverlap + 50.52(± 22.47). D: ΔT1, where tMCAo = 42.83 (± 13.88) * ΔT1 – 93.03 (± 83.17). E: ΔT2 where tMCAo = 24.41 (± 7.2) * ΔT2 + 64.74 (± 30.86).
58x44mm (300 x 300 DPI)